Zeolite Materials Hot Paper

DOI: 10.1002/anie.201311324

A Uniformly Oriented MFI Membrane for Improved CO_2 Separation**

Ming Zhou, Danil Korelskiy, Pengcheng Ye, Mattias Grahn, and Jonas Hedlund*

Abstract: *Membrane separation of CO_2 from natural gas, biogas, synthesis gas, and flu gas is a simple and energy-efficient alternative to other separation techniques. But results for CO_2-selective permeance have always been achieved by randomly oriented and thick zeolite membranes. Thin, oriented membranes have great potential to realize high-flux and high-selectivity separation of mixtures at low energy cost. We now report a facile method for preparing silica MFI membranes in fluoride media on a graded alumina support. In the resulting membrane straight channels are uniformly vertically aligned and the membrane has a thickness of 0.5 μm. The membrane showed a separation selectivity of 109 for CO_2/H_2 mixtures and a CO_2 permeance of 51×10^{-7} mol m^{-2} s^{-1} Pa^{-1} at −35 °C, making it promising for practical CO_2 separation from mixtures.*

The challenge of developing effective separation and purification technologies that have much smaller energy footprints is greater for carbon dioxide (CO_2) than for other gases.[1] In addition to its involvement in climate change, CO_2 is an impurity in precombustion natural gas (CO_2/CH_4), biogas (natural gas produced from biomass), synthesis gas (CO_2/H_2, the main source of hydrogen in refineries), and postcombustion flue gas (CO_2/N_2).[2] The separation of CO_2 from these mixtures is of great interest from an environmental and energy perspective: Effectively capturing CO_2 from power plants can have a positive impact on reducing greenhouse gas emissions. CO_2 separation from synthesis gas generated from biomass is necessary to achieve a suitable composition of the gas prior to the synthesis of fuels such as methanol. Removal of CO_2 from biogas and natural gas is necessary since CO_2 reduces the heating value, causes pipe corrosion, and occupies volume in the pipeline. Membrane technology combines high energy efficiency with simple process equipment, which plays a key role in making the separation economically feasible. Polymeric membranes are already commercially available for natural gas upgrading;[3] however, polymeric membranes generally suffer from low resistance to contaminants, physical aging, and membrane plasticization at high pressures of CO_2.[4]

Zeolites are amongst the most widely reported physical adsorbents for CO_2 capture in the patent and journal literature.[5] They can bring their intrinsic properties, such as well-defined molecular-sized pores, high thermal, chemical, and mechanical stabilities, and hydrophobicity/philicity, into the membrane. Ideally, zeolite membranes should be large-scale ordered and defect-free, exhibiting high thermal stability, selectivity, and permeability.[6] Zeolite SAPO-34,[7,8] FAU,[9,10] DDR,[11] T-type,[12] Ba-ZSM-5,[13] and MFI[14–17] membranes have been reported for CO_2/CH_4, CO_2/N_2, and CO_2/H_2 separations. These membranes either have demonstrated high selectivity for CO_2 over other gas molecules with low permeability owing to the thickness of the zeolite films and the random arrangement of zeolite crystals in the membrane, or have demonstrated high flux of CO_2 with moderate selectivity due to defects present in the membranes. High silica MFI or pure silica MFI zeolite membranes with 5.6×5.3 Å straight channels vertical (*b*-oriented) to the porous support have demonstrated very promising separations of xylene isomers.[18–20] The separation occurs by a molecular sieving mechanism, because *p*-xylene and *o*-xylene molecules are roughly 0.58 nm and 0.68 nm in size, respectively. These *b*-oriented MFI membranes were supported by homemade porous α-Al_2O_3 or silica disks, using trimer-tetrapropylammonium hydroxide (TPAOH) or tetraethylammonium hydroxide (TEAOH)/$(NH_4)_2SiF_6$ as structure-directing agents (SDAs), and have fewer defects, such as pinholes or cracks, than previously reported MFI membranes with random, *c*-, or [h0h]-orientations. Here in this study, for the first time a uniformly *b*-oriented MFI membrane is produced on a commercially available α-Al_2O_3 disk with a graded pore structure; TPA + F is used as an SDA. The as-prepared MFI membrane shows a significantly low level of defects and an improved separation performance for CO_2/H_2 mixtures.

It is well known that zeolite crystals prepared at neutral pH using F^- as the mineralizing agent contain fewer defects[21] and are more hydrophobic.[22] There are only a few reports on the preparation of zeolite films using F^- as the mineralizing agent. Examples are the preparations of zeolite Beta[23] and MFI[24] films on silicon wafers and porous alumina supports, respectively. However, these films were synthesized from randomly oriented seed layers or grown in unfavorable gels, which resulted in films with no or only weak orientation of the crystals.

The close-packed and uniformly *b*-oriented MFI seed ($1.2\times1.0\times0.45$ μm^3) monolayer was produced on a glass plate by previously reported methods[25] (Figure 1 a,d). The seed layer was immersed into TPA + F gel with a tetraethyl orthosilicate (TEOS)/TPAOH/H_2O/HF molar composition of 1:0.2:200:0.2, the reaction was carried out at 150 °C for 24 h. The SEM images of the MFI film are shown in Figure 1 b,e. The surface morphology was smooth and continuous and showed considerable in-plane growth along the *c*-axis; the surface crystals typically have dimensions of 10 μm

[*] Dr. M. Zhou, D. Korelskiy, P. Ye, M. Grahn, Prof. J. Hedlund
Chemical Technology, Luleå University of Technology
Porsön Campus, 97187 Luleå (Sweden)
E-mail: ming.zhou@ltu.se

[**] We acknowledge Bio4Energy and the Swedish Foundation for Strategic Research for financially supporting this work. The Knut and Alice Wallenberg Foundation is acknowledged for financially supporting the Magellan SEM instrument.

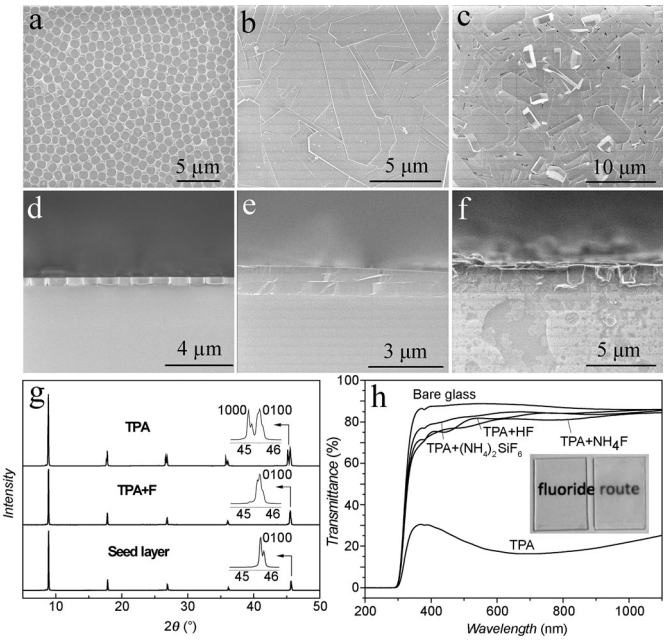

Figure 1. Top (a–c) and side (d–f) view SEM images of glass-supported MFI seed layers with crystal sizes of $1.2\times1.0\times0.45\ \mu m^3$ (a, d), after growth in TPA + F gel (b, e) and in clear TPA solution (c, f) at 150 °C for 24 h. g) Corresponding XRD patterns. h) Transmittance spectra of glass plates coated with MFI films, which were prepared by growth of seed layer in TPA + F gels and in TPA solution (as indicated), and a photograph of the glass plates (insert).

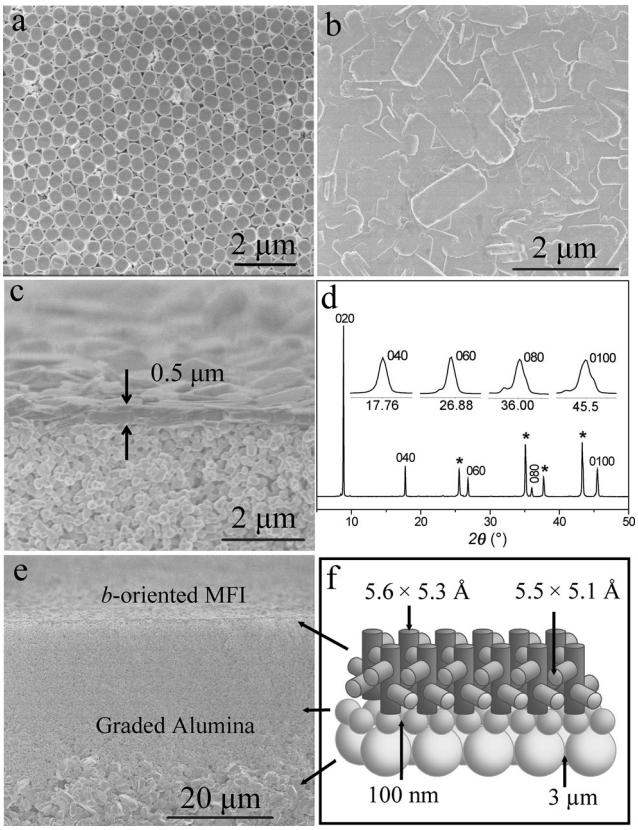

Figure 2. a) SEM image of an MFI seed layer with a crystal size of $0.5\times0.45\times0.2\ \mu m^3$ on a porous alumina support. b–e) SEM images and XRD pattern of *b*-oriented MFI membrane after growth of the seed layer in TPA + F gel at 100 °C for 48 h. f) Representation of oriented MFI channel systems on a graded alumina support.

along *c*-axis and 2–3 μm along *a*-axis, which is in agreement with their typical long coffin shape. The thickness of this film was 1.0 μm. In the same synthesis solution but without added HF, the seed layer underwent out-of-plane fast growth to form a film with a thickness of 2.5 μm after 24 h of growth at 150 °C (Figure 1 c,f). Corresponding XRD patterns of seed layer and MFI films are shown in Figure 1 g. The MFI film grown in TPA + F gel was *b*-oriented; five distinct peaks at 8.82°, 17.74°, 26.78°, 36.00°, and 45.48° were attributed to (020), (040), (060), (080), and (0100) reflections. The MFI film grown in TPA solution is *a*- and *b*-oriented as evidenced by five new peaks observed at 8.75°, 17.61°, 26.58°, 35.72°, and 45.10°, which were attributed to (200), (400), (600), (800) and (1000) reflections, consistent with the SEM observations. The MFI films grown in TPA + F gel appeared quite transparent, which might be attributed to their thin and smooth structure and there was no additional crystal form on the back side of the glass plate. In contrast, the MFI films prepared in TPA solution seemed semitransparent; their film surface was irregular and the back side of the glass plate was also covered with an MFI film by in situ growth, as illustrated by transmittance spectra and the insert photograph in Figure 1 h.

MFI crystals with a smaller size ($0.5\times0.45\times0.2\ \mu m^3$) were organized in a *b*-oriented monolayer on the surface of a porous alumina disk with a diameter of 25 mm by previously reported methods[26–28] (Figure 2 a). The seeded alumina support was immersed in a TPA + F gel with a SiO_2/TPAOH/H_2O/HF composition of 1:0.12:60:0.12, using colloidal SiO_2 30 % as the silica source; the reaction was carried out at 100 °C in oil bath under reflux for 48 h. The resulting MFI membrane showed primarily in-plane growth with surface crystals typically possessing a length of 1.8 μm along the *c*-axis and 0.6 μm along the *a*-axis (Figure 2 b). The thickness of this membrane was 0.5 μm (Figure 2 c). In the corresponding XRD pattern (Figure 2 d) the five distinct peaks at 8.82°, 17.74°, 26.78°, 36.00°, and 45.48° were attributed to (020), (040), (060), (080), and (0100) reflections, which confirmed that the membrane was *b*-oriented. The four peaks marked by asterisks (*) on the XRD trace indicate peaks of the α-alumina support. The side view of the supported film at lower magnification revealed its hierarchical structure (Figure 2 e), which displayed three sets of pores with sizes in the sequence of 5.6 × 5.3 Å, 100 nm, and 3 μm, respectively (Figure 2 f).

Methods have been developed previously for evaluating the defects in membranes; they include: measuring the ratio of single-gas permeances,[6] permporometry,[29] and fluorescence confocal optical microscopy.[30] Figure 3 a shows the *n*-hexane/helium adsorption-branch permporometry data for the *b*-oriented MFI membrane produced in this study and compares it with the data from a randomly oriented MFI membrane with same thickness prepared in an earlier study.[31] At $p/p_0=0$, the helium permeance is $67\times10^{-7}\ mol\,m^{-2}\,s^{-1}\,Pa^{-1}$ for the randomly oriented membrane and $64\times10^{-7}\ mol\,m^{-2}\,s^{-1}\,Pa^{-1}$ for the *b*-oriented membrane. When *n*-hexane is added to the feed ($p/p_0=0.01$), the zeolite

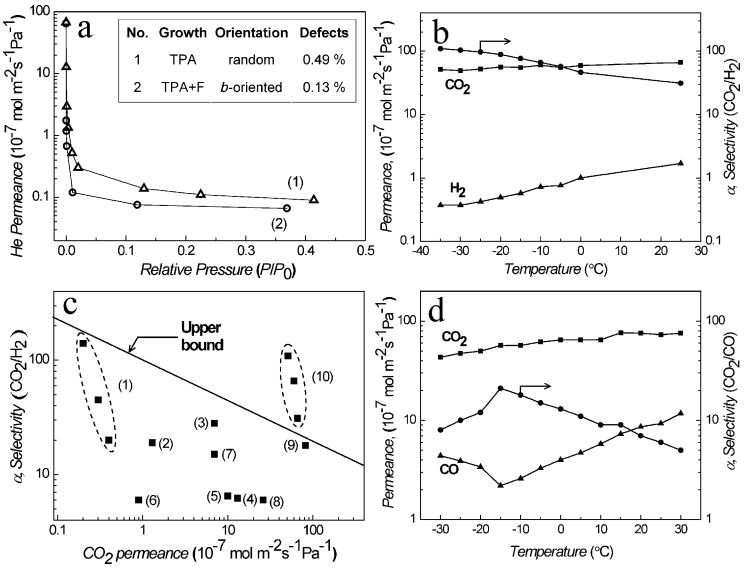

Figure 3. a) Permporometry patterns for randomly and *b*-oriented MFI membranes; insert summarizes the defect areas of the two membranes. b, d) Results for the separation of 50:50 CO_2/H_2 (b) and CO_2/CO (d) gas mixtures with the *b*-oriented MFI membrane. c) Comparison of selectivity versus CO_2 permeance for the *b*-oriented MFI membrane, the randomly oriented MFI membrane, and other types of zeolite membranes for CO_2/H_2 gas mixture separation; the straight line denotes the upper bound of zeolite membranes for CO_2/H_2 separation, data in the dotted oval labeled 10 are the results for the *b*-oriented MFI membrane from this study. See Table 1 for an explanation of points 1–10.

pores are blocked and the helium permeance is dramatically reduced. Any remaining helium flow at this point is permeating through defects larger than about 1.6 nm. For randomly and *b*-oriented membranes, the helium permeance decreased by 99.2 % and 99.8 %, respectively, when the relative pressure of *n*-hexane increased from 0 to 0.01. Table 1 summarizes the total amount of defects, which account for 0.49 % and 0.13 % of the total surface areas of the randomly and *b*-oriented MFI membranes, respectively. This indicates the *b*-oriented membrane produced in this study has fewer defects than the randomly oriented membrane with 0.5 μm thickness reported earlier by our group.[32] The addition of F^- is not the only reason that the defect area is reduced: the MFI membrane grown in fluoride gel with random orientation has a defect area of 0.24 %.[24] The uniform *b*-orientation contributes to the decrease of the defect area further to 0.13 %.

Table 1: Explanation of data for points 1–10 in Figure 3.

No.	*T* [°C]	Membrane	Thickness [μm]	Orientation	Ref.
1	−20 to 23	SAPO-34	5	random	[8]
2	60	FAU	15–18	random	[9]
3	35	FAU (NaY)	3	random	[10]
4	25	Ba-ZSM-5	0.55	random	[13]
5	60	MFI (modified)	0.55	random	[36]
6	25	MFI	7	random	[15]
7	20	MFI	40–50	*c*, (*h*0*l*)	[14]
8	25	MFI	0.5	random	[24]
9	25	MFI	0.7	random	[17]
10	−35 to 25	MFI	0.5	*b*	this work

Separation selectivity and permeance are two important parameters used to evaluate membrane separation performance. The MFI membrane used in this study separate CO_2/H_2 mixture by a competitive adsorption[33] and diffusion[15] mechanism. Figure 3 b,d shows separation results for 50:50 CO_2/H_2 and 50:50 CO_2/CO mixtures for 0.5 μm thick *b*-oriented MFI membrane. The membrane showed highest CO_2/H_2 selectivity at −35 °C, with a value of 109. This is because zeolites are selective to CO_2 over H_2 at lower temperatures due to strong CO_2 adsorption and blocking of H_2 permeation. The selectivity drops with increasing temperature: at −10 °C the observed separation selectivity was 66 and at 25 °C the selectivity was about 31. The CO_2 permeances were very high in the range of $51–66 \times 10^{-7}$ mol m^{-2} s^{-1} Pa^{-1}. The membrane showed the highest CO_2/CO selectivity of 21 at −15 °C with a CO_2 permeance of 57×10^{-7} mol m^{-2} s^{-1} Pa^{-1}. It is important that the flux of the membrane is high, so that the required membrane area can be reduced and industrial applications economically more affordable. In the molecular sieving separation of H_2/CO_2 mixture the (kinetic diameters of H_2 and CO_2 are 0.289 nm and 0.33 nm, respectively), the highest reported H_2 permeance was 20×10^{-7} mol m^{-2} s^{-1} Pa^{-1} for a silica membrane[34] and ca. 2×10^{-7} mol m^{-2} s^{-1} Pa^{-1} for a graphene oxide membrane.[35]

An upper bound can be used to compare the separation performance of the new membrane with that of previously reported membranes. Figure 3 c shows a comparison of our *b*-oriented MFI membrane with previously reported zeolite membranes with random orientations for the separation of CO_2/H_2 mixtures. The selectivity of the *b*-oriented MFI membrane is above the upper bound and its separation performance is superior to that of the randomly oriented SAPO-34, FAU, Ba-ZSM-5, and MFI membranes.

In summary, a *b*-oriented zeolite MFI membrane with a thickness of 0.5 μm was fabricated on a commercially available α-alumina support by a facile TPA-fluoride route. This membrane showed CO_2/H_2 and CO_2/CO mixture separation performances that are higher than those of the state-of-the-art random-orientation zeolite membranes; this makes it attractive for practical CO_2 separation from mixtures.

Experimental Section

Synthesis of MFI seeds: Plate-shaped MFI crystals with crystal sizes of $1.2 \times 1.0 \times 0.45$ μm^3 and $0.5 \times 0.45 \times 0.2$ μm^3 were synthesized from mixtures with a TEOS/TPAOH/H_2O molar composition of 1:0.2:100 but with different hydrolysis time. Two identical solutions were shaken at room temperature for 1 day and 7 days, respectively, before they were subjected to hydrothermal treatment at 130 °C for 9 h under constant stirring. Crystals synthesized from both solutions were purified by repetitive centrifugation and re-dispersion in distilled deionized water and freeze-dried before use.

Assembly of monolayer: Monolayers of *b*-oriented MFI crystals ($1.2 \times 1.0 \times 0.45\ \mu m^3$) were assembled on glass plates by rubbing the powders of freeze-dried crystals onto the surfaces using a Nitrile-gloved finger.[25] The porous-alumina-supported MFI seed layers ($0.5 \times 0.45 \times 0.2\ \mu m^3$) were produced by dynamic interfacial assembly[26] or by polymer-mediated assembly.[27,28]

Growth of membranes: The glass-supported seed layer was immersed in a gel with a TEOS/TPAOH/H_2O/HF molar composition 1:0.2:200:0.2 and the reaction was carried out in autoclave at 150 °C for 24 h. The alumina-supported seed layer was subjected to hydrothermal treatment in a gel with a SiO_2/TPAOH/H_2O/HF molar composition of 1:0.12:60:0.12, using colloidal SiO_2 30 % as the silica source; the reaction was carried out in an oil bath at 100 °C under reflux for 48 h. After synthesis, the membranes were rinsed with a 0.2 M ammonia solution and dried at 50 °C over night. Calcination was then performed at 500 °C for 6 h, with a heating rate of 0.2 °C min^{-1} and a cooling rate of 0.3 °C min^{-1}.

Permporometry and separations: After calcination, the membrane was mounted in a stainless steel cell sealed with graphite gaskets and copper gaskets. Then, the measurement of *n*-hexane/helium adsorption-branch permporometry was performed. Prior to the separation experiments, the membrane was dried for 6 h at 300 °C in a flow of nitrogen. CO_2/H_2 (1:1) and CO_2/CO (1:1) mixtures were fed to the membrane at total feed pressure of 9 bar. The total permeate pressure was kept at 1 bar. The composition in both feed and permeate streams is known from GC analysis. No sweep gas was used.

Received: December 31, 2013
Published online: March 3, 2014

Keywords: carbon dioxide · gas separation · membranes · thin films · zeolites

[1] P. Nugent, Y. Belmabkhout, S. D. Burd, A. J. Cairns, R. Luebke, K. Forrest, T. Pham, S. Q. Ma, B. Space, L. Wojtas, M. Eddaoudi, M. J. Zaworotko, *Nature* **2013**, *495*, 80 – 84.
[2] D. M. D'Alessandro, B. Smit, J. R. Long, *Angew. Chem.* **2010**, *122*, 6194 – 6219; *Angew. Chem. Int. Ed.* **2010**, *49*, 6058 – 6082.
[3] S. Basu, A. L. Khan, A. Cano-Odena, C. Liu, I. F. J. Vankelecom, *Chem. Soc. Rev.* **2010**, *39*, 750 – 768.
[4] Y. Xiao, B. T. Low, S. S. Hosseini, T. S. Chung, D. R. Paul, *Prog. Polym. Sci.* **2009**, *34*, 561 – 580.
[5] S. Choi, J. H. Drese, C. W. Jones, *ChemSusChem* **2009**, *2*, 796 – 854.
[6] M. Yu, R. D. Noble, J. L. Falconer, *Acc. Chem. Res.* **2011**, *44*, 1196 – 1206.
[7] S. G. Li, J. L. Falconer, R. D. Noble, *Adv. Mater.* **2006**, *18*, 2601 – 2603.
[8] M. Hong, S. Li, J. L. Falconer, R. D. Noble, *J. Membr. Sci.* **2008**, *307*, 277 – 283.
[9] J. Caro, M. Noack, *Microporous Mesoporous Mater.* **2008**, *115*, 215 – 233.
[10] K. Kusakabe, T. Kuroda, K. Uchino, Y. Hasegawa, S. Morooka, *AIChE J.* **1999**, *45*, 1220 – 1226.
[11] S. Himeno, T. Tomita, K. Suzuki, K. Nakayama, K. Yajima, S. Yoshida, *Ind. Eng. Chem. Res.* **2007**, *46*, 6989 – 6997.
[12] X. L. Zhang, L. F. Qiu, M. Z. Ding, N. Hu, F. Zhang, R. F. Zhou, X. S. Chen, H. Kita, *Ind. Eng. Chem. Res.* **2013**, *52*, 16364 – 16374.
[13] J. Lindmark, J. Hedlund, *J. Membr. Sci.* **2010**, *360*, 284 – 291.
[14] H. L. Guo, G. S. Zhu, H. Li, X. Q. Zou, X. J. Yin, W. S. Yang, S. L. Qiu, R. Xu, *Angew. Chem.* **2006**, *118*, 7211 – 7214; *Angew. Chem. Int. Ed.* **2006**, *45*, 7053 – 7056.
[15] M. Kanezashi, Y. S. Lin, *J. Phys. Chem. C* **2009**, *113*, 3767 – 3774.
[16] M. P. Bernal, J. Coronas, M. Menéndez, J. Santamaría, *AIChE J.* **2004**, *50*, 127 – 135.
[17] L. Sandström, E. Sjöberg, J. Hedlund, *J. Membr. Sci.* **2011**, *380*, 232 – 240.
[18] Z. P. Lai, G. Bonilla, I. Diaz, J. G. Nery, K. Sujaoti, M. A. Amat, E. Kokkoli, O. Terasaki, R. W. Thompson, M. Tsapatsis, D. G. Vlachos, *Science* **2003**, *300*, 456 – 460.
[19] T. C. T. Pham, H. S. Kim, K. B. Yoon, *Science* **2011**, *334*, 1533 – 1538.
[20] T. C. T. Pham, T. H. Nguyen, K. B. Yoon, *Angew. Chem.* **2013**, *125*, 8855 – 8860; *Angew. Chem. Int. Ed.* **2013**, *52*, 8693 – 8698.
[21] J. L. Guth, H. Kessler, R. Wey, *Stud. Surf. Sci. Catal.* **1986**, *28*, 121 – 128.
[22] K. Zhang, R. P. Lively, J. D. Noel, M. E. Dose, B. A. McCool, R. R. Chance, W. J. Koros, *Langmuir* **2012**, *28*, 8664 – 8673.
[23] L. Tosheva, M. Hölzl, T. H. Metzger, V. Valtchev, S. Mintova, T. Bein, *Mater. Sci. Eng. C* **2005**, *25*, 570 – 576.
[24] H. Zhou, D. Korelskiy, E. Sjöberg, J. Hedlund, *Microporous Mesoporous Mater.* **2014**, in press.
[25] J. S. Lee, J. H. Kim, Y. J. Lee, N. C. Jeong, K. B. Yoon, *Angew. Chem.* **2007**, *119*, 3147 – 3150; *Angew. Chem. Int. Ed.* **2007**, *46*, 3087 – 3090.
[26] M. Zhou, J. Hedlund, *J. Mater. Chem.* **2012**, *22*, 3307 – 3310.
[27] M. Zhou, J. Hedlund, *J. Mater. Chem.* **2012**, *22*, 24877 – 24881.
[28] B. Q. Zhang, M. Zhou, X. F. Liu, *Adv. Mater.* **2008**, *20*, 2183 – 2189.
[29] J. Hedlund, D. Korelskiy, L. Sandstrom, J. Lindmark, *J. Membr. Sci.* **2009**, *345*, 276 – 287.
[30] G. Bonilla, M. Tsapatsis, D. G. Vlachos, G. Xomeritakis, *J. Membr. Sci.* **2001**, *182*, 103 – 109.
[31] D. Korelskiy, T. Leppajarvi, H. Zhou, M. Grahn, J. Tanskanen, J. Hedlund, *J. Membr. Sci.* **2013**, *427*, 381 – 389.
[32] J. Hedlund, J. Sterte, M. Anthonis, A. J. Bons, B. Carstensen, N. Corcoran, D. Cox, H. Deckman, W. De Gijnst, P. P. de Moor, F. Lai, J. McHenry, W. Mortier, J. Reinoso, *Microporous Mesoporous Mater.* **2002**, *52*, 179 – 189.
[33] T. C. Golden, S. Sircar, *J. Colloid Interface Sci.* **1994**, *162*, 182 – 188.
[34] R. M. de Vos, H. Verweij, *Science* **1998**, *279*, 1710 – 1711.
[35] H. Li, Z. N. Song, X. J. Zhang, Y. Huang, S. G. Li, Y. T. Mao, H. J. Ploehn, Y. Bao, M. Yu, *Science* **2013**, *342*, 95 – 98.
[36] J. Lindmark, J. Hedlund, *J. Mater. Chem.* **2010**, *20*, 2219 – 2225.

